05,08

Demultiplexing of spin-waves in the structure ferromagnetic film|ferroelectric|magnonic crystal

© M.A. Morozova[1], O.V. Matveev[1], Yu.P. Sharaevsky[1], S.A. Nikitov[1,2]

[1] Saratov National Research State University,
Saratov, Russia
[2] Kotelnikov Institute of Radio Engineering and Electronics, Russian Academy of Sciences,
Moscow, Russia
E-mail: mamorozovama@yandex.ru

Received October 23, 2024
Revised October 26, 2024
Accepted October 27, 2024

The article covers the principle of multiplexing/demultiplexing of microwave signals based on the structure ferromagnetic film|ferroelectric|magnonic crystal. The formation of five band gaps, i. e. spin-wave stopbands, has been found in such a structure. It is shown that, the signal exits through different ports of the structure depending on the frequency, i. e. channels are frequency-separated. The frequency range supplied to this port is determined by the dielectric permittivity of the ferroelectric layer (which is determined by the applied electric field) and the magnitude of the magnetic field applied to the ferromagnetic layers.

Keywords: magnonics, multiferroics, frequency separation of channels, spin current.

DOI: 10.61011/PSS.2024.11.60093.275

1. Introduction

Multiferroic materials in which the properties of spin-waves can be controlled using not only a magnetic field, but also an electric field are among the most promising materials in which spin-wave propagation is possible [1,2]. Artificial multiferroics include ferromagnetic and ferroelectric layers and exhibit both properties characteristic of each layer individually and new properties associated with the interaction of magnetic and electrical subsystems [3,4]. Electromagnetic waves in the ferroelectric are strongly slowed down in case of high dielectric permittivity of the ferroelectric, which depends on the applied electric field. Hybrid electromagnetic spin-waves (HESW) occur in this case in the structure ferromagnetic film|ferroelectric (FF|FE) at frequencies close to the frequency of phase synchronism between electromagnetic waves (EMW) and magnetostatic waves (MSW) [5,6].

In turn, periodic structures based on multiferroic materials such as multiferroic magnonic crystals open up great possibilities for wave control compared to homogeneous structures due to the existence of Bragg resonances. Bragg resonances in such structures are observed at wavelengths satisfying both the Bragg condition and the condition of phase synchronism of magnetostatic and electromagnetic waves [7–9]. Band gaps (BG), i. e. stopbands, are formed in the HESW spectrum at frequencies corresponding to Bragg resonances [9,10]. This effect allows considering such structures as the basic element of filtering of a spin-wave signal with electric and magnetic control [7,8,10–12]. However, it should be expected that the presence of band gaps and the asymmetry of the structure (for example, for a structure with a magnonic crystal (MC, MC) — FF|FE|MC) will open up broader possibilities for using such a structure for functional signal processing. The possibility of frequency separation of the signal between the layers of the demultiplexing structure is considered in this paper.

It should be noted that a single MC also allows the signal to be discriminated at frequencies outside the BG. However, the signal at the BG frequencies exits through the input port of the structure in this case, and it is difficult to separate it from the input signal. Demultiplexing is also possible in the structure MC-1|dielectric|MC-2 as shown in [13]. However, the mechanism is fundamentally different in this case: the signal enters the second layer at the BG frequencies and is reflected from it, while, as expected, signal in the structure FF|FE|MC cannot be pumped to the second layer (MC in this case) at the BG frequency, since the propagation conditions are more „favorable“ (there is no lattice) in the FF layer. As a result, separated signals propagate at different frequencies in the same layer in different directions and exit through different ports in the structure MC-1|dielectric|MC-2. Separated signals will propagate in different layers (FF and MC, respectively) in the same direction at different frequencies in the structure FF|FE|MC and exit through different ports, which allows for a more efficient signal separation.

It is also known that there is also the possibility of frequency separation of channels in a layered structure based on FF-1|dielectric|FF-2 [14,15]. However, the mechanism of frequency separation in this case is fundamentally different from the mechanism for periodic structures and is also related to the dependence of the pumping length on frequency. The disadvantage of using the structure FF-1|dielectric|FF-2, compared with the FF|FE|MC structure, is that only signals for which the pumping length differs by half will be effectively separated. The use of a Y-shaped waveguide also allows for frequency separation of signals due to the action of an electric current in a metal substrate, however, it is necessary to change the direction of the magnetic field for frequency separation in this case [16]. A demultiplexer based on magnonic transfer between two chains of magnetic clusters connected by a resonant structure has been proposed in Ref. [17,18]. It was demonstrated in Ref. [19] that it is possible to generate and control a configurable nanochannel using voltage-controlled magnetic anisotropy. An on/off switch is presented, which is the basis for implementing demultiplexers with multiple outputs that filter spin-waves with the same or different frequencies, depending on the need, as well as with or without an external magnetic field. A four-channel demultiplexer based on magnetic waveguides is theoretically proposed in Ref. [20], the design of which includes a system of resonators. A magnonic demultiplexer was proposed in Ref. [21], the action of which is based on Fano resonances. Magnonic multiferroid crystals also have resonant properties, which means they can be useful in creating demultiplexers.

Wave equations and dispersion relations are obtained for HESW in the structure FF|FE|MC. The dispersion characteristics and transmission coefficients of the HESW are calculated. A mechanism for multiplexing/demultiplexing a spin-wave signal based on such a structure has been identified. The possibility of controlling the frequency division of channels using an electric field applied to the FE and a magnetic field applied to the FF and MC has been established.

2. The structure model and basic relationships

To begin with, let us consider a layered structure consisting of ferromagnetic films FF-1 and FF-2 with thickness $d_{1,2}$ with saturation magnetization $M_{0_{1,2}}$ separated by a FE layer with thickness D_{FE}. An external magnetic field $\overline{H}_0$ is applied tangentially to the surface of the films along the axis x, and an external electric field with strength $\overline{E}$ is applied to the FE layer with dielectric permittivity ε along the axis z. The structure is infinite in the direction of the axes x and y (Figure 1).

The wave equation for the HESW in a single FF with a thickness d with a saturation magnetization M_0 loaded with

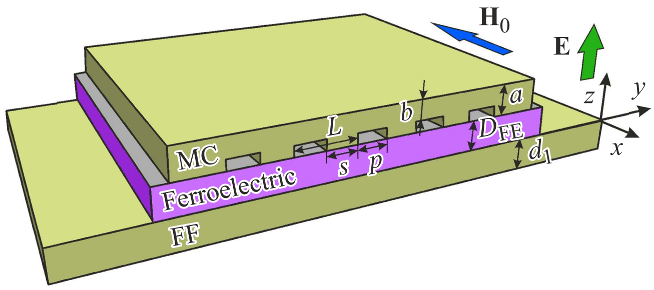

Figure 1. The diagram of the structure FF|FE|MC.

a FE layer has the following form [9]:

$$\frac{\partial^4 m}{\partial t^4} - \omega_\perp^2 \frac{\partial^2 m}{\partial t^2} + \omega_M^2 d\left(-jS\,\frac{1}{2}\,\frac{\partial^3}{\partial t^2 \partial y} - \frac{c^2}{\varepsilon D_{\mathrm{FE}}}\,\frac{\partial^2}{\partial y^2}\right)m$$

$$- j\,\frac{2c^2}{\varepsilon D_{\mathrm{FE}}}\,\frac{\partial m}{\partial y}\left(\frac{\partial^2 m}{\partial t^2} - \omega_\perp^2\right) + \frac{\varepsilon d \omega_M}{c^2}\left(\frac{\partial m}{\partial y}\right)^{-1}$$

$$\times \frac{\partial^2}{\partial t^2}\left(-\frac{\partial m}{\partial t} + j\left(\omega_H + \frac{\omega_M}{2}\right)\right) = 0, \qquad (1)$$

where $m = m_x/M_0$ is the normalized high-frequency component of magnetization, $S = \pm 1$ (the sign „–" refers to a wave propagating in the positive direction x, the sign „+" refers to a wave propagating in the negative direction x), $\omega_\perp^2 = \omega_H(\omega_H + \omega_M)$, $\omega_H = \gamma H_0$, $\omega_M = 4\pi\gamma M_0$, γ is gyromagnetic ratio, c is the speed of light. The last term in the equation (1)

$$\theta = \frac{\varepsilon d \omega_M}{c^2}\left(\frac{\partial m}{\partial y}\right)^{-1}\frac{\partial^2}{\partial t^2}\left(-\frac{\partial m}{\partial t} + j\left(\omega_H + \frac{\omega_M}{2}\right)\right)$$

describes the relationship between a surface magnetostatic wave (SMSW) in FF and an electromagnetic wave (EMW) in FE.

We will assume that two bound HESW are excited in a structure consisting of two FF separated by a layer of FE, one of which (HESW-1) propagates in the structure FF-1|FE, and the second (HESW-2) propagates in the structure FF-2|FE. HESW are connected only through the FE layer. In this case, the wave equations for each HESW with envelope amplitudes $m_{1,2}$, without any connection between them, will have the form similar to equation (1), up to the substitution of $d \to d_{1,2}$, $\omega_M \to \omega_{M_{1,2}}$, respectively. Then the last term in equation (1), written for HESW-1, has the form

$$\theta_1 = \frac{\varepsilon d_1 \omega_{M_1}}{c^2}\left(\frac{\partial m}{\partial y}\right)^{-1}\frac{\partial^2}{\partial t^2}\left(-\frac{\partial m}{\partial t} + j\left(\omega_H + \frac{\omega_{M_1}}{2}\right)\right)$$

and determines the effect of the SMSW propagating in the FF-1 on the EMW in the FE (as well as the reverse effect of the EMW on the MSW). In the structure FF-1|FE|FF-2 on EMW in FE will also have an impact on MSW propagating in FF-2. The magnitude of such an effect will be determined by the magnitude of the relationship between the SMSW in FF-2 and the EMW in FE. The relationship between SMSW in FF-2 and EMW in FE, in turn, is described by the last term in equation (1), written for HESV-2 and having the form

$$\theta_2 = \frac{\varepsilon d_2 \omega_{M_2}}{c^2}\left(\frac{\partial m}{\partial y}\right)^{-1}\frac{\partial^2}{\partial t^2}\left(-\frac{\partial m}{\partial t} + j\left(\omega_H + \frac{\omega_{M_2}}{2}\right)\right).$$

Thus, the mutual influence of HESV-1 and HESV-2 will be determined by the superposition of these terms in each of the equations for HESV-1 and HESV-2.

The system of wave equations for the structure FF-1|FE|FF-2 will have the following form taking into account the assumptions made and the equation (1):

$$\begin{aligned}
&\frac{\partial^4 m_{1,2}}{\partial t^4} - \omega^2_{\perp_{1,2}}\frac{\partial^2 m_{1,2}}{\partial t^2}\\
&+ \omega^2_{M_{1,2}} d_{1,2}\left(-jS\,\frac{1}{2}\,\frac{\partial^3}{\partial t^2 \partial y} - \frac{c^2}{\varepsilon D_{\mathrm{FE}}}\frac{\partial^2}{\partial y^2}\right) m_{1,2}\\
&- j\,\frac{2c^2}{\varepsilon D_{\mathrm{FE}}}\frac{\partial m_{1,2}}{\partial y}\left(\frac{\partial^3 m_{1,2}}{\partial t^2} - \omega^2_{\perp_{1,2}}\right) + \frac{\varepsilon d_{1,2}\omega_{M_{1,2}}}{c^2}\\
&\times\left(\frac{\partial m_{1,2}}{\partial y}\right)^{-1}\frac{\partial^2}{\partial t^2}\left(-\frac{\partial m_{1,2}}{\partial t} + j\left(\omega_H + \frac{\omega_{M_{1,2}}}{2}\right)\right)\\
&+ \frac{\varepsilon d_{2,1}\omega_{M_{2,1}}}{c^2}\left(\frac{\partial m_{2,1}}{\partial y}\right)^{-1}\\
&\times\frac{\partial^2}{\partial t^2}\left(-\frac{\partial m_{2,1}}{\partial t} + j\left(\omega_H + \frac{\omega_{M_{2,1}}}{2}\right)\right) = 0. \qquad (2)
\end{aligned}$$

A limiting transition is performed at $\varepsilon \to 0$ as follows from equation (2), and the equations for FF-1 and FF-2 turn out to be decoupled. This is attributable to the fact that in this case, the HESW in the FE layer cannot propagate, the connection between the MSW through the FE layer disappears, and thus, the SMSW propagate independently in FF-1 and FF-2. It should be noted that the connection between the SMSW in FF-1 and FF-2 through microwave electromagnetic fields was not taken into account when constructing this model, but the connection through the FE layer was taken into account. This type of connection is predominant with a large thickness of FE ($D_{\mathrm{FE}} > 10^2\,\mu$m) and large values of ε ($\varepsilon > 10^3$), which will be considered further.

Let us assume at the next stage that a periodic system of grooves with a depth Δ has been created on the surface of the FF-2, spaced with a period L, p is the width of the grooves, s is the width of the bars, a is the thickness of the film in the area of the bars, b is the thickness of the film in the area of the grooves. In this case, the FF-2 is a MC. The MC thickness can be represented as a periodic function [22]:

$$d_{1,2} = d_{0_{1,2}}\left[1 + \delta_{d_{1,2}}\cos\left(\frac{2\pi}{L}\,y\right)\right], \qquad (3)$$

where for MC-2 $\delta_d = \frac{2\Delta}{\pi d_{0_2}}\sin\left(\frac{\pi s}{L}\right)$, $d_{0_2} = b_2 + \frac{\Delta s}{L}$ is the effective thickness of MC. For FF, we have $\Delta = 0$, then $\delta_d = 0$ and $d_{0_1} = d_1$.

Solving the wave equation (2) using (3) can be represented as a sum of spatial harmonics [23]: $m = \sum_{n=-\infty}^{\infty} A_n \exp[jk_n y]$, where A_n are the complex harmonic amplitudes, k_n is the constant distribution. Only the zero harmonics of direct waves ($n = 0$) and „-1“ are the wave harmonics of waves reflected from spatial inhomogeneities ($n = -1$) in the first Brillouin zone $0 \le k_n L \le 2\pi$, $n = \ldots - 2, -1, 0, 1, 2\ldots$. In this case, the solution of the wave equation (1) can be represented as the sum of direct and reflected waves:

$$m = A\exp[j(\omega t - k_0 y)] + B\exp[j(\omega t + k_{-1} y)], \qquad (4)$$

where A and B are slowly varying complex amplitudes of the envelopes of the forward and reflected waves, k_0 is the propagation constant of the zero harmonic, k_{-1} refers to „-1-th“ harmonic, $\omega = 2\pi f$ is the frequency of the input signal (carrier frequency). The propagation constants k_0 and k_{-1} are related by the Bragg condition: $k_{-1} = -k_0 + 2\pi/L$.

Substituting (3) and (4) into the system (2), we obtain a system of equations for the envelopes of direct and reflected waves in the structure under study in the form

$$\begin{cases}
j\left(\dfrac{\partial A_{1,2}}{\partial t} + V_{1,2}\dfrac{\partial A_{1,2}}{\partial y}\right) + \eta_{1,2_0}A_{1,2} + \chi_{1,2_0}A_{2,1}\\
\qquad + \kappa_{1,2_0}B_{1,2} + \vartheta_{1,2_0}B_{2,1} = 0,\\
j\left(\dfrac{\partial B_{1,2}}{\partial t} - V_{1,2}\dfrac{\partial B_{1,2}}{\partial y}\right) + \eta_{1,2_{-1}}B_{1,2} + \chi_{1,2_{-1}}B_{2,1}\\
\qquad + \kappa_{1,2_{-1}}A_{1,2} + \vartheta_{1,2_{-1}}A7A_{2,1} = 0.
\end{cases} \qquad (5)$$

The equations for quantities with the index „1“ will describe the HESW in the FF, and the equations for quantities with the index „2“ will describe the HESW in the MC. $V_{1,2}$ are group velocities in equations (5); $\chi_{1,2_0}$ are coupling coefficients between the direct wave in FF-1 (MC-2) and the direct wave in MC-2 (FF-1); $\chi_{1,2_{-1}}$ are coupling coefficients between reflected wave in FF-1 (MC-2) and reflected wave in MC-2 (FF-1); $\kappa_{1,2_0}$ are coupling coefficients between direct wave in FF-1 (MC-2) and the reflected wave in FF-1 (MC-2); $\kappa_{1,2_{-1}}$ are coupling coefficients between the reflected wave in FF-1 (MC-2) and the direct wave in FF-1 (MC-2); $\vartheta_{1,2_0}$ are coupling coefficients between the direct wave in FF-1 and the reflected wave in MC-, as well as between the direct wave in MC-2 and the reflected wave in FF-1; $\vartheta_{1,2_{-1}}$ are coupling coefficients between the reflected wave in FF-1 and the direct wave in MC-2, as well as between the reflected wave in MC-2 and the direct wave in FF-1; $\eta_{1,2_0}$ when equated to zero, represent the normalized dispersion relations for direct MSW in homogeneous films 1 and 2; $\eta_{1,2_{-1}}$ when equated to zero, represent the normalized dispersion ratios for reflected MSW in homogeneous films 1 and 2.

The coefficients in (5) have the form

$$\left.\begin{aligned}
V_{1,2} &= \frac{\omega_{M_{1,2}}^2 d_{0_{1,2}}}{4\omega^3}\left(\frac{\omega^2}{2}+\frac{2c^2k_{0,-1}}{\varepsilon D_{\mathrm{FE}}}\right) + \frac{2c^2}{4\omega^3\varepsilon D_{\mathrm{FE}}}(\omega^2+\omega_{\perp_{1,2}}^2)\\
\eta_{1,2_{0,-1}} &= \frac{\Omega^{\mathrm{FE}}_{1,2_{0,-1}}}{4\omega^3}\\
\chi_{1,2_{0,-1}} &= \chi_{1,2} = -\frac{\varepsilon\omega_{M_{2,1}}d_{0_{1,2}}\omega^2}{c^2k_0}\left(\omega+\omega_H+\frac{\omega_{M_{2,1}}}{2}\right)\\
\kappa_{2_0} &= \frac{\delta_d}{8\omega^3}\,\omega_{M_2}d_{0_{1,2}}\left(\frac{c^2\omega_{M_2}}{\varepsilon D_{\mathrm{FE}}}\,k_{-1}^2-\frac{\omega_{M_2}}{2}\,\omega^2k_{-1} - \frac{\varepsilon\omega^2}{c^2k_{-1}}\left(\omega+\omega_H+\frac{\omega_{M_2}}{2}\right)\right)\\
\kappa_{2_{-1}} &= \frac{\delta_d}{8\omega^3}\,\omega_{M_2}d_{0_{1,2}}\left(\frac{c^2\omega_{M_2}}{\varepsilon D_{\mathrm{FE}}}\,k_0^2-\frac{\omega_{M_2}}{2}\,\omega^2k_0 - \frac{\varepsilon\omega^2}{c^2k_0}\left(\omega+\omega_H+\frac{\omega_{M_2}}{2}\right)\right)\\
\vartheta_{1_0} &= \frac{\delta_d}{2}\,\chi_{1_{-1}},\quad \vartheta_{1_{-1}} = \frac{\delta_d}{2}\,\chi_{1_0}\\
\kappa_{1_{0,-1}} &= 0,\quad \vartheta_{2_{0,-1}} = 0,
\end{aligned}\right\}, \tag{6}$$

where the components $\Omega^{\mathrm{FE}}_{1,2_0}$, equated to zero, represent the dispersion relations for the straight line and are determined by the ratio $\Omega^{\mathrm{FE}}_{1,2_0} = \Omega_{0_{1,2}}\Omega_0^E - \frac{\varepsilon d_{1,2}\omega_{M_{1,2}}d_{0_{1,2}}\omega^2}{c^2k_0} \times \left(\omega+\omega_H+\frac{\omega_{M_{1,2}}}{2}\right)$ at $kd_{1,2} \ll 1$. $\Omega_0^E = -\omega^2 + c^2\frac{2k}{\varepsilon D_{\mathrm{FE}}}$, equated to zero, is the dispersion relation for the first EMW mode ($i = 1$) in an isolated FE at $k \to k_0$ [6.24]. $\Omega_{1,2_0} = \omega^2 - \omega_{\perp_{1,2}}^2 - \frac{\omega_{M_{1,2}}^2 kd_{0_{1,2}}}{2}$, equated to zero, is the dispersion relation for the SMSW in isolated FF at $k \to k_0$ [25,26]. The components $\Omega^{\mathrm{FE}}_{1,2_{-1}}$, equated to zero, represent the dispersion relations for the reflected HESW and are determined by a similar ratio at $k \to k_{-1}$.

It is possible to obtain a dispersion relation for HESW in the structure of the FF|FE|MC from the condition of compatibility of the system (5) with coefficients (6) in the following form

$$\begin{bmatrix} \eta^{\mathrm{FE}}_{1_0} & \kappa^{\mathrm{FE}}_{1_0} & \chi^{\mathrm{FE}}_{1_0} & \vartheta^{\mathrm{FE}}_{1_0}\\ \kappa^{\mathrm{FE}}_{1_{-1}} & \eta^{\mathrm{FE}}_{1_{-1}} & \vartheta^{\mathrm{FE}}_{1_{-1}} & \chi^{\mathrm{FE}}_{1_{-1}}\\ \chi^{\mathrm{FE}}_{2_0} & \vartheta^{\mathrm{FE}}_{2_0} & \eta^{\mathrm{FE}}_{2_0} & \kappa^{\mathrm{FE}}_{2_0}\\ \vartheta^{\mathrm{FE}}_{2_{-1}} & \chi^{\mathrm{FE}}_{2_{-1}} & \kappa^{\mathrm{FE}}_{2_{-1}} & \eta^{\mathrm{FE}}_{2_{-1}} \end{bmatrix} = 0. \tag{7}$$

A dispersion relation can be obtained for HESW in the structure FF-1|FE|FF-2 by limit transition from the ratio (7). In this case, assuming $\delta_d = 0$ (since $\Delta = 0$), we have $\kappa^{\mathrm{FE}}_{1,2_{0,-1}} = \vartheta^{\mathrm{FE}}_{1,2_{0,-1}} = 0$, $\eta^{\mathrm{FE}}_{1,2_{-1}} = 0$, and the variance ratio (7) will take the form

$$\begin{vmatrix} \eta^{\mathrm{FE}}_{1_0} & \chi^{\mathrm{FE}}_2\\ \chi^{\mathrm{FE}}_1 & \eta^{\mathrm{FE}}_{2_0} \end{vmatrix} = 0. \tag{8}$$

3. Dispersion characteristics

Let's consider the mechanism of hybridization of EMW with SMSW in the structure FF-1|FE|FF-2. Figure 2 shows the dispersion characteristic of the first EMW mode ($i = 1$) of the isolated FE layer (dotted line), as well as the law of dispersion of the EMW in isolated FF-1 and FF-2 (dashed lines). The mechanism of hybridization in this case is as follows: first of all, the hybridization of EMW and SMSW in a thick film of FF-1 (at point A). This is explained by the fact that the maxima of the magnetic fields of the EMW are located on the upper surfaces of the FF-1 and FF-2, resulting in the most effective interaction between the EMW and SMSW occurs in a thick film of FF-1 (when the SMSW propagates in the opposite direction, the hybridization sequence will be reversed). As a result of hybridization, a primary HESW is formed (dashed curves), the phase velocity of its low-frequency branch turns out to be close to the velocity of the PMW in the thin film FF-2, and additional rapping of the dispersion curves occurs (at point B). The resulting HESW, which arises from the interaction of EMW with FF-1 and FF-2, has three branches of dispersion (solid curves): fast HESW (HESW-b, branch *1*) and *2* slow HESW (HESW-m1, branch *21* and HESW-m2, branch *22*).

It should be noted that the exact dispersion relation for HESW in the structure FF-1|FE|FF-2 was obtained in

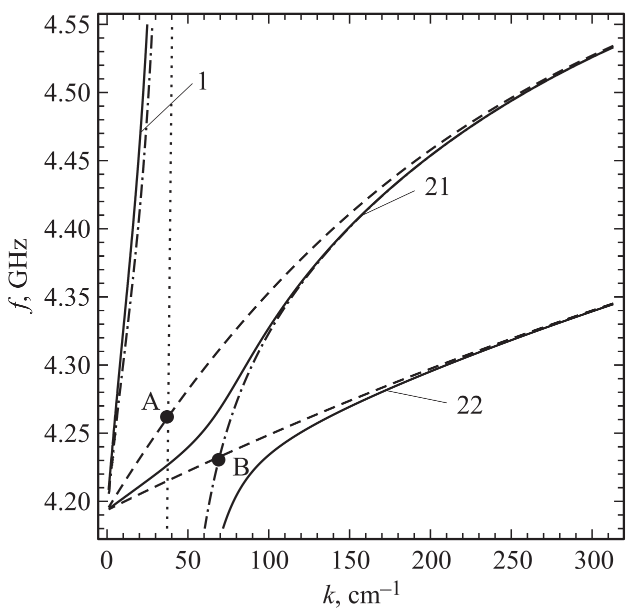

Figure 2. Dispersion characteristics of HESW in the structure FF-1|FE|FF-2 (solid curves), HESW-1 (dashed-dotted curves), EMW in the isolated layer of FE (dotted curve), PMW in the structure FF-1|FF-2 (dotted curves) ($d_1 = 26\,\mu$m, $a_2 = 12\,\mu$m, $D_{\mathrm{FE}} = 500\,\mu$m, $\varepsilon = 3000$, $H_0 = 860$ Oe, $M_0 = 140$ G).

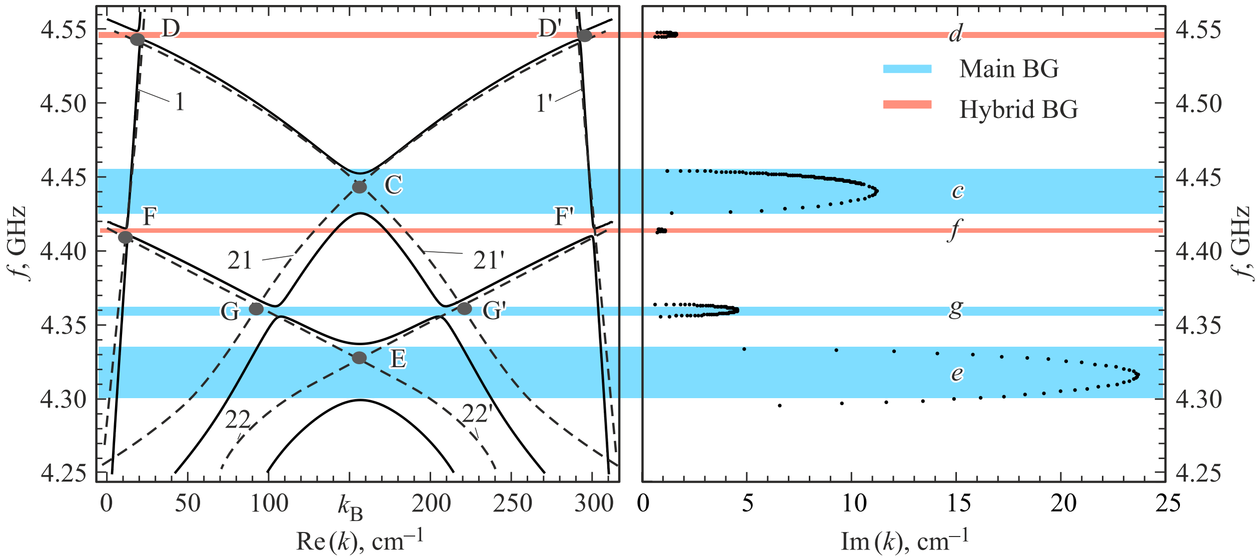

Figure 3. Dispersion characteristics of HESW in MC-1|FE|MC-2 in the absence of a connection between direct and reflected waves (dotted curves) and in the presence of a connection between waves (solid curves) ($d_1 = 26\,\mu$m, $\Delta_1 = 2\,\mu$m, $a_2 = 1\,\mu$m, other parameters as in Figure 2).

Ref. [27] based on the solution of Maxwell's equations and the crosslinking of components of electric and magnetic fields at the interface. The mechanism of wave hybridization in the structure FF-1|FE|FF-2 based on the constructed model is consistent with the results of Ref. [27]. However, there is a quantitative discrepancy between the results obtained and the results presented in this paper by no more than 10 MHz and 5 cm^{-1}. This difference is explained by a number of approximations and simplifying assumptions made during the construction of this model.

Figure 3 shows the dispersion characteristics of the HESW in the structure FF|FE|MC, calculated by the ratio (7), in the absence of a connection between direct and reflected waves (dotted curves) and in the presence of a connection between the waves (solid curves). The real values of the wave numbers k are plotted along the horizontal axis in the left side of the figure, imaginary values k are plotted in the right side of the figure.

It can be seen from the variance dependencies in Figure 3 that there are 8 points of intersection of dotted curves (points E, G, G′, F, F′, C, D, D′). The conditions of phase synchronism will be fulfilled at these points when different types of waves interact.

1. Interaction of direct and reflected HESW-m2 (branches *22* and *22′*, point E), a band gap c is formed.

2. Interaction of direct and reflected HESW-m1 (branches *21* and *21′*, point C), a band gap e is formed.

3. Interaction of HESW-m1 and HESW-m2 (branches *21* and *22′*, point G; branches *22* and *21′*, point G′), a band gap g is formed.

4. Interaction of the straight HESW-b and HESW-m1 (branches *1* and *21′*, point D; branches *1′* and *21*, point D′), a band gap d is formed.

5. Interaction of the HESW-b and HESW-m2 lines (branches *1* and *22′*, point F; branches *1′* and *22*, point F′), a band gap f is formed.

Thus, five band gaps are formed in the structure FF|FE|MC, three of which are formed by the interaction of slow HESW-m (bands c, e, g are shown in blue). We will call these bands as the main ones, since the mechanism of their formation is similar to the mechanism of formation of the BG in the structure MC-1|dielectric|MC-2 [22]. The third and fourth bands are formed due to the interaction of direct fast HESW-b and reflected slow HESW-m, or direct slow HESW-m and reflected fast HESW-b (bands d, f are shown in red). We will call these bands as hybrid band gaps, since they are not formed in structure MC-1|dielectric|MC-2, and the mechanism of their formation is attributable to interaction with the fast branch of HESV-b, which is formed solely through the hybridization of EMW and SMSW.

4. The principle of signal multiplexing/demultiplexing

The system (5) with coefficients (6) can be used to describe the wave evolution of the envelope amplitudes in the structure FF|FE|. The initial and boundary conditions were set as

$$A_{1,2}(y,0) = 0,\ B_{1,2}(y,0) = 0,\ A_1(0,t) = A_{01} f(t),$$
$$A_2(0,t) = A_{02} f(t),\ B_{1,2}(l,t) = 0, \qquad (9)$$

where A_{01} and A_{02} are the amplitudes of the pulses supplied to MC-1 and MC-2, $f(t)$ describes the shape of the input pulse, in particular, for the input pulse of Gaussian shape

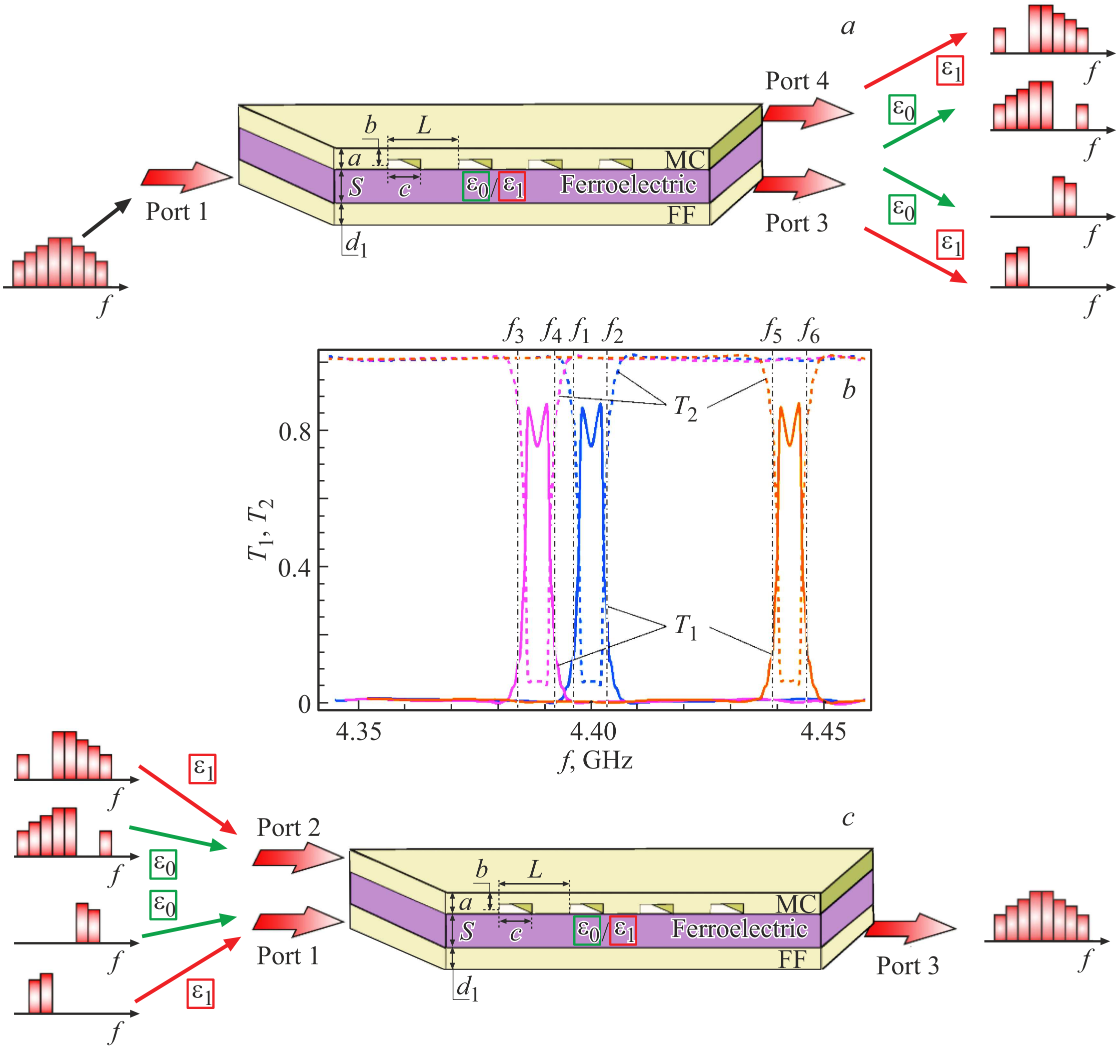

Figure 4. *a*) The scheme of the studied structure, the principle of demultiplexing based on the structure FF|FE|MC. *b*) The dependence of the FF-1 transmission coefficients (T_1, solid curves) and MC (T_2, dotted curves) on the frequency at different values of the external magnetic field and the dielectric permittivity of the ferroelectric (at $H_0 = 860$ Oe, $\varepsilon = 3000$ — blue curves, at $H_0 = 860$ Oe, $\varepsilon = 5000$ — pink curves, at $H_0 = 880$ Oe, $\varepsilon = 3000$ — brown curves). *c*) The principle of multiplexing based on the structure FF|FE|MC.

$f(t) = \exp[-(\frac{t-\tau_0}{\tau_{\text{imp}}})^2]$; τ_{imp} and τ_0 are the duration and delay of the input pulse, respectively. The pulse duration was chosen so that the width of its frequency spectrum was less than the band gap.

The structure FF|FE|MC can be considered as a four-port structure with one input port and four output ports (ports 1–4) (see Figure 4, *a*). Then the transmission coefficients of FF-1 (T_1) — determining the proportion of power output through FF-1 (port 2) and MC-2 (T_2) — determining the proportion of input power output through MC-2 (port 4), determined by the ratios

$$T_{1,2} = \frac{\int_0^{T_{\max}} |A_{1,2}(l,t)|^2 dt}{\int_0^{T_{\max}} |A_1(0,t) + A_2(0,t)|^2 dt}, \qquad (10)$$

where $T_{\max}$ is the observation time.

Let's choose the length of the structure l to be a multiple of half the length of the power transfer between the layers of the structure and investigate the dependence of the transmission coefficients on the frequency of the input signal. Let the input signal be supplied to the FF-1 (port 1, as shown by the red arrow in Figure 4, *a*), let us set $A_{01} \neq 0$, $A_{02} = 0$ in the relations (9).

Figure 4, *b* shows the dependence of the transmission coefficients of FF-1 (T_1, solid curves) and MC-2 (T_2, dotted curves) on the frequency of the input signal. It can be seen that transmission coefficient for MC-2 T_2 at $\varepsilon = 3000$ and $H_0 = 860$ Oe has a characteristic minimum at frequencies $f_1 < f < f_2$ corresponding to the band gap (blue dotted curve). A maximum transmission coefficient is observed for FF-1 T_1 (blue solid curve) at the same frequencies. Consequently, the signal entering the FF-1 at the frequencies lying in the BG is not pumped to the MC-2, but passes through the FF-1 without distortion. The described behavior of the transmission coefficients will lead to the separation of the signal by the output ports of the structure MC|FE|FF. The signal at frequencies lying in the BG ($f_1 < f < f_2$) will exit the FF-1, i.e. through port 2. The signal will exit MC-2 at frequencies outside the band gap $f < f_1$ and $f < f_2$, i.e. through port 4 (this is attributable to the fact that the signal is completely pumped to MC-2 at the selected length). The hybrid zone shifts down in frequency at $\varepsilon = 5000$ (pink solid curves). Thus, only a signal with frequencies in the range $f_3 < f < f_4$ will be output through port 2. The signal at frequencies outside this range $f < f_3$ and $f < f_4$ will exit through port 4. The transmission coefficient of MC-2 at a different value of the magnetic field $H_0 = 880\,\mathrm{Oe}$ and $\varepsilon = 3000$ is shown by a brown solid curve. In this case, the band gap shifts up in frequency. Therefore, a signal with a frequency in the range $f_5 < f < f_6$ will exit through port 2, a signal with frequencies outside this range $f < f_5$ and $f < f_6$ will exit through port 4.

Thus, the signal exits through different ports of the structure depending on the frequency, i.e. the studied structure allows for frequency channel separation — demultiplexing. The range of frequencies received by this port is determined by the value of the dielectric permittivity of the ferroelectric (which depends on the electric field applied to the ferroelectric) and the value of the magnetic field applied to the ferromagnetic layers.

On the other hand, we obtain both signals at the output of the FF-1 (port 2) by applying a signal at the frequency of the band gap to the FF-1 (port 1), and a signal with a frequency outside the band gap to the MC-2 (port 3). Consequently, the studied structure allows for frequency channel combination — multiplexing (Figure 4, *c*). Any range of frequencies can be supplied to the FF in this case, and it is necessary to select the value of the dielectric permittivity of the FE and magnetic field for performing the multiplexing function, in such a way that the selected range coincides with the BG of the studied structure.

The described effects allow considering the structure FF|FE|MC as a basic element for frequency multiplexing/demultiplexing of signals with dual control — magnetic and electric. This element allows separating input signals by frequency, outputting them through different output ports, and combining signals at different frequencies supplied to different input ports, outputting them from one output port. Multiplexing/demultiplexing devices, in turn, are one of the basic elements of telecommunications and, in particular, are widely used in computer networks and fiber optics [28,29].

5. Conclusion

A model describing the dispersion characteristics of the HESW in the structure FF|FE|MC is built. It is shown that five band gaps are formed in such a structure, three of which are formed as a result of the interaction of direct and reflected slow HESW in each layer (main band gaps). Two band gaps are formed as a result of the interaction of direct fast HESW-b and reflected slow HESW-m in each layer (hybrid band gaps). The hybrid bandgaps become wider with the increase of the dielectric permittivity ε. A dual control (by electric and magnetic fields) of the density of the band gaps and the characteristics of the BG in the HESW spectrum is possible in the structure FF|FE|MC.

The signal exits through different ports of the structure depending on the frequency, i.e. the studied structure allows frequency channel separation- demultiplexing. The frequency range applied to the ports is determined by the dielectric permittivity of the ferroelectric (which depends on the magnitude of the electric field) and the magnitude of the magnetic field applied to the ferromagnetic layers. The studied structure also allows combining signals with different frequencies on the same port — multiplexing. Any frequency range can be supplied to the FF in this case, and it is necessary to select the dielectric permittivity of the FE and the magnetic field for implementing the multiplexing function so that the selected range coincides with the band gap of the structure.

The described effects allow considering the structure FF|FE|MC as a basic element for frequency multiplexing/demultiplexing of magnetically and electrically controlled signals.

Funding

This study was supported by the Russian Science Foundation (project № 23-29-000759, https://rscf.ru/project/23-29-000759/).

Conflict of interest

The authors declare that they have no conflict of interest.

References

[1] V. Garcia, M. Bibes, A. Barthélémy. Comptes Rendus Physique **16**, *2*, 168 (2015).
[2] A.K. Pyatakov, A.K. Zvezdin. Phys. — Uspekhi, **55**, *6*, 557 (2012).
[3] N.X. Sun, G. Srinivasan. SPIN **2**, *3*, 1240004 (2012).
[4] C.-W. Nan, M.I. Bichurin, S. Dong, D. Viehland, G. Srinivasan. J. Appl. Phys. **103**, *3*, 031101 (2008).
[5] V.B. Anfinogenov, T.N. Verbitskaya, P.E. Zilberman. PZhTF **12**, *8*, 454, (1986). (in Russian).
[6] O.G. Vendik, B.A. Kalinikos, S.I. Miteva Izv. vuzov. Radioelectronika **24**, *9*, 52 (1981). (in Russian).
[7] Al.A. Nikitin, An.A. Nikitin, A.V. Kondrashov, A.B. Ustinov, B.A. Kalinikos, E. Lähderanta. J. Appl. Phys. **122**, *15*, 153903 (2017).
[8] I.A. Ustinova, A.A. Nikitin, A.B. Ustinov. Tech. Phys. **61**, *3*, 473 (2016).
[9] M.A. Morozova, O.V. Matveev, D.V. Romanenko, S.A. Nikitov. JETP **137**, *4*, 432 (2023).
[10] M.A. Morozova, S.V. Grishin, A.V. Sadovnikov, D.V. Romanenko, Yu.P. Sharaevskii, S.A. Nikitov. IEEE Trans. Magn. **51**, *11*, 2802504 (2015).

[11] A.V. Drozdovskii, A.A. Nikitin, A.B. Ustinov, B.A. Kalinikos. Tech. Phys. **59**, *7*, 1032 (2014).
[12] A.B. Ustinov, B.A. Kalinikos. Tech. Phys. Lett. **40**, *7*, 568 (2014).
[13] M.A. Morozova, O.V. Matveev, D.V. Romanenko, A.V. Trukhanov, A.M. Mednikov, Yu.P. Sharaevskii, S.A. Nikitov. J. Magn. Magn. Mater. **508**, 166836 (2020).
[14] H. Sasaki, N. Mikoshiba. J. Appl. Phys. **52**, *5*, 3546 (1981).
[15] H. Sasaki, N. Mikoshiba. Electron. Lett. **15**, *6*, 172 (1979).
[16] K. Vogt, F.Y. Fradin, J.E. Pearson, T. Sebastian, S.D. Bader, B. Hillebrands, A. Hoffmann, H. Schultheiss. Nature Commun. **5**, *1*, 3727 (2014).
[17] H. Al-Wahsh, B. Djafari-Rouhani, L. Dobrzynski, A. Akjouj. Surf. Sci. **602**, *10*, 1795 (2008).
[18] H. Al-Wahsh. Eur. Phys. J. B **76**, *3*, 445 (2010).
[19] B. Rana, Y. Otani. Phys. Rev. Appl. **9**, *1*, 014033 (2018).
[20] A. Mouadili, A. Akjouj, E. El Boudouti, L. Dobrzynski. JETP **130**, *6*, 859 (2020).
[21] A. Mouadili, E.H. El Boudouti, A. Akjouj, H. Al-Wahsh, B. Djafari-Rouhani, L. Dobrzynski. AIP Adv. **9**, *3*, 035011 (2019).
[22] M.A. Morozova, A.Yu. Sharaevskaya, A.V. Sadovnikov, S.V. Grishin, D.V. Romanenko, E.N. Beginin, Yu.P. Sharaevskii, S.A. Nikitov. J. Appl. Phys. **120**, *22*, 223901 (2016).
[23] D. Marcuse. Theory of Dielectric Optical Waveguides. Academic Press (1974).
[24] V.E. Demidov, B.A. Kalinikos, P. Edenhofer. J. Appl. Phys. **91**, *12*, 10007 (2002).
[25] A. Prabhakar, D.D. Stancil. Spin Waves. Theory and applications. Springer (2009).
[26] A.G. Gurevich, G.A. Melkov. Magnetization, Oscillations and Waves. CRC-Press, London (1996).
[27] An.A. Nikitin, A.B. Ustinov, V.V. Vitko, Al.A. Nikitin, A.V. Kondrahov, P. Pirro, E. Lähderanta, B.A. Kalinikos, B. Hillebrands. J. Appl. Phys. **122**, *1* (2017).
[28] J. Torrejon, M. Riou, F. Abreu Araujo, S. Tsunegi, G. Khalsa, D. Querlioz, P. Bortolotti, V. Cros, K. Yakushiji, A. Fukushima, H. Kubota, S. Yuasa, M.D. Stiles, J. Grollier. Nature **547**, *7664*, 428 (2017).
[29] G.P. Agrawal. Lightwave Technology: Telecommunication Systems. John Wiley & Sons, Inc. (2005).

Translated by A.Akhtyamov